

# Vortex Generator Jets—Means for Flow Separation Control

James P. Johnston\*

Stanford University, Stanford, California 94305

and

Michihiro Nishi\*

Kyushu Institute of Technology, Tobata, Kitakyushu 804, Japan

Stalled regions (zones of detached or separated flow sometimes followed by reattachment) in a turbulent boundary layer may be eliminated by a technique called the vortex-generator-jet (VGJ) method. The method employs spanwise arrays of small, skewed, and pitched jets from holes in the surface. Low-speed air-flow experiments are described which 1) demonstrate that the VGJ method creates longitudinal (streamwise) vortices in the boundary layer downstream of the jet holes similar to the vortices behind solid vortex generators and 2) show that the cross-stream mixing associated with these vortices is effective in reduction and elimination of stalled regions.

## Nomenclature

|            |   |
|------------|---|
| $C_f$      | = wall skin friction coefficient, $2\tau_w/\rho U_\infty^2$         |
| $C_p$      | = wall static pressure coefficient, $2(p - p_{ref})/\rho U_{ref}^2$ |
| $D$        | = jet hole diameter   |
| $p$        | = wall static pressure  |
| $p_{ref}$  | = wall static pressure at $x=0$ , station L1                        |
| $U_{ref}$  | = freestream velocity at $x=0$ , station L1                         |
| $U_\infty$ | = local freestream velocity   |
| $u$        | = streamwise mean velocity  |
| $V_j$      | = jet mean speed  |
| $VR$       | = $V_j/U_{ref}$ , ratio of jet speed to reference freestream speed  |
| $x$        | = streamwise distance from station L1                               |
| $y$        | = distance normal to wall   |
| $z$        | = spanwise distance from wall center line                           |
| $\delta$   | = boundary-layer thickness  |
| $\phi$     | = pitch angle of jet hole   |
| $\theta$   | = skew angle of jet hole relative to $x$ direction                  |

## Introduction

A COMMONLY used method for flow separation control employs small vortex generators (rectangular or delta shaped winglets), which are imbedded in a turbulent boundary layer ahead of a line of flow separation.<sup>1</sup> Spanwise arrays of vortex generators are often placed along a wing upstream of the flap hinge or inside the lip of a jet engine inlet diffuser. The longitudinal vortices generated in the boundary layer increase cross-stream mixing of streamwise momentum and suppress or eliminate separation.

This paper introduces and explores a different and rarely, if ever, used method for production of the weak longitudinal vortices needed for separation control. Small jets blown through holes in the solid surface can generate longitudinal streamwise vortices in a boundary layer, and these vortices act to increase cross-stream mixing of streamwise momentum. The surface holes are pitched at an angle to the surface and inclined relative to the main flow direction. They are arrayed along the surface much like ordinary vortex generator winglets. We have designated this method the VGJ (vortex-generator-jet) method.

The VGJ method was first examined some years ago by Wallis<sup>2,4</sup> and Wallis and Stuart<sup>3</sup> in Australia, primarily for the purpose of delaying shock-induced separation of turbulent boundary layers. A more recent study by Ball<sup>5</sup> on stall suppression for jet-engine-inlet diffusers employed VGJs alone and together with solid generators. Both studies show that the method has potential. How much potential is not clear at this point because we have yet to learn of any working system that actually employed the technique, and much basic information on the method is yet to be obtained.

Fixed, solid-vortex generators have the advantages of simplicity, ruggedness, and low cost. Their disadvantages are that 1) they cannot be used in active stall control, a technology now being adopted for highly maneuverable fighter aircraft, and 2) they add parasitic drag in flow situations where stall suppression is not needed, e.g., steady cruise conditions. With some added complexity and cost, the VGJ method can obviate both of these disadvantages. For example, if the flow requirements for the jets is a very small fraction of the total jet engine flow, then compressor bleed air would suffice to power the system and produce the VGJs. Air-flow control, either proportional or simple on/off, is readily accomplished by the use of electrically actuated valves in the air supply lines. With jets off there is no parasitic drag, but on command they may be rapidly and continuously actuated to provide the correct degree of separation control.

The potential applications of VGJ systems are numerous for external flow over aircraft and missiles. Internal flows in diffusers can also be improved and pressure losses reduced. For example, the system might have application to shorter, lighter jet engine inlet diffusers,<sup>5</sup> and possibly VGJ's might be used with appropriate flow direction sensors and a feedback control system to suppress surge and rotating stall in compressors of jet engines.

Because so little is currently known about generation of longitudinal vortices in a turbulent boundary layer by small pitched and skewed wall jets, the goals of the research underlying this paper are 1) to explore the parameter space of this effect in a set of simple, well-controlled experiments, 2) to demonstrate the effectiveness of the VGJ method for suppression of turbulent boundary-layer separation, and 3) to provide engineering design data (e.g., minimum jet speeds, sizes, and angles) for effective utilization. The objectives of the paper are to present some data on a simple configuration (jets pitched at 45 deg to the surface and skewed at 90 or 180 deg to the flow in several configurations), which demonstrates that the jets can create streamwise vortices, and that they indeed suppress turbulent boundary-layer stall.

Received March 31, 1989; revision received Aug. 17, 1989. Copyright © 1989 American Institute of Aeronautics and Astronautics, Inc., All rights reserved.

\*Professor, Mechanical Engineering Department. Member AIAA.

### Scope and Approach

Two kinds of results are described. They are based on two sets of experiments: Set A, a demonstration that vortices are generated in a turbulent boundary layer of nearly constant freestream speed for various jet velocities (jet speeds) where they issue from the wall,  $V_j$ , equal to and lower than local freestream speed, and set B, experiments on the effectiveness of the VGJs to control stall (separation and reattachment) when a strong adverse pressure gradient is applied to the layer.

In both cases, a two-dimensional, turbulent boundary layer, growing on a smooth flat wall of a low-speed wind tunnel (inlet air speed,  $U_{ref}$  15 m/s, at room temperature and pressure), was used. The test section is 61 cm wide between parallel side walls, and 12.7 cm high from the nozzle exit to the flange downstream of station L1. A side view of the tunnel's working section is shown in Fig. 1. The top-wall shape was adjusted to control the pressure gradient along the test wall. Boundary-layer removal at the beginning of the adjustable top wall together with arrays of small, delta-shaped, solid-vortex generators, along the side walls, between L1 and L2, and across the top wall at L2, prevented separation on these surfaces when strong adverse pressure gradients were applied between stations L2 and L4 to cause the test surface layer to separate.

The boundary layer was turbulent downstream of the trip in the nozzle. Without the VGJs operating (jetoff situation), it was 1.5 cm thick at  $x=0$ , station L1, where its momentum thickness Reynolds number was 1400. In addition, it was two dimensional over almost the whole 61 cm of span ( $z$  direction) between the parallel side walls of the tunnel.

The holes for the VGJs are 6.35 mm in diameter. As seen in Fig. 2, they were drilled at a pitch angle of 45 deg through each of six smooth plugs that span the test section wall on 10.2 cm centers at the L1 location. Air pumped to the plenum behind the plugs was metered, and the mean jet speed determined to an accuracy of  $\pm 0.2$  m/s. The plugs can be positioned at any skew angle. For the experiments of set A, the skew was set alternately at  $\pm 90$  deg for the six plugs with the two on either side of the centerline at  $z = \pm 5.1$  cm having their jet holes directed at each other [the  $JP = \pm 90$  (in) configuration shown in Fig. 3]. For set B experiments with boundary-layer separation, four other jet configurations were used. Three configurations with skew set at  $\pm 90$  deg displaced sym-

metrically about  $z=0$ , the central plane, one with all six jets set at  $+90$  deg (not symmetrical) and one case with the skew at 180 deg to the downstream direction, out of the page in the downstream view designated  $JP=180$  in Fig. 3.

### Results

#### Set A

Experiments to demonstrate that the flow from the VGJs can produce longitudinal vortices in the turbulent boundary layer well downstream of the jet-hole location, station L1, are described first. Here the top wall was maintained at a constant  $y$  distance of 12.7 cm above the test surface, and as a consequence the boundary layer grew downstream in a weak negative pressure gradient. For practical purposes, local freestream speed  $U_\infty$  was close to  $U_{ref}$  of 15 m/s at all stations along the surface. Data were obtained using a slender stagnation pressure probe (0.89 mm tip diam, 76 mm long from tip to stem) mounted on a two-axis traversing unit that could move normal to the wall from  $y=0$  to 10 cm and over  $z \pm 20$  cm of the spanwise axis, a distance that included four of the six VGJ's. The traverse unit may be installed over any of the L stations. Two types of results are deduced with this probe/traverse system: 1) profiles of the skin friction coefficient  $C_f$  at two streamwise stations, L2 and L4 (probe tip at  $x=22.9$  and 83.8 cm downstream of the VGJ hole location, respectively), and 2) mean velocity profiles  $u(y)$  at selected spanwise locations at station L2. The  $C_f$  values were deduced by the Preston tube method using the Patel<sup>6</sup> correlation.

The spanwise profiles or skin friction coefficient are presented for stations L2 and L4 in Figs. 4a and 4b, respectively. There are three curves on each figure. Curve A is the case of now blowing (jetoff), and  $C_f$  is nearly constant across the span. The other two curves (B and C) show significant local peaks and valleys in  $C_f$  associated with four of the spanwise jets. The latter two cases correspond to strong jet blowing,  $VR=1$  and weaker jet blowing at  $VR=0.4$ . The weaker jets create weaker disturbances as expected.

The shapes of the peaks and valleys in the spanwise  $C_f$  profiles and their locations and magnitudes with respect to the jets which cause them are good diagnostic tools. The observed profile shapes in Figs. 4a and 4b are very similar to the spanwise  $C_f$  profiles one expects to be associated with longitudinal vortices imbedded in a boundary layer. Good examples are provided by Pauley and Eaton,<sup>7,8</sup> who made detailed studies of the vortices generated by small vortex generators in a turbulent boundary layer, which was very similar to the one used in the current study. In their results (see Fig. 16 in Ref. 7 and

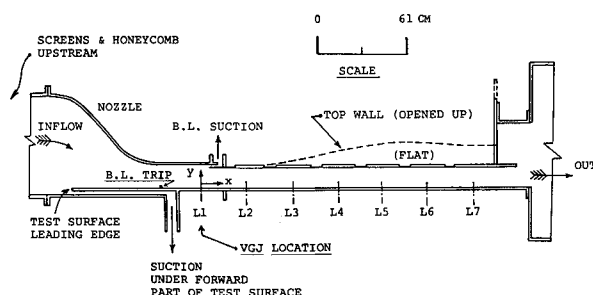


Fig. 1 Wind tunnel test section; constant width of 61 cm; VGJs across section L1,  $x=0$ .

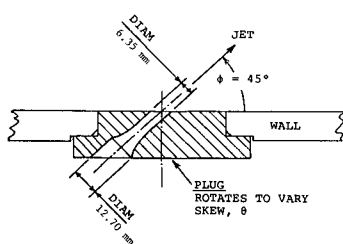


Fig. 2 VGJ wall plug detail; over operating Reynolds ( $Re$ ) number range of 2500 to 6000, nozzle discharge coefficient varies from 0.84 to 0.90 (laminar);  $Re$  based on mean speed  $V_j$  and hole diameter, 6.35 mm.

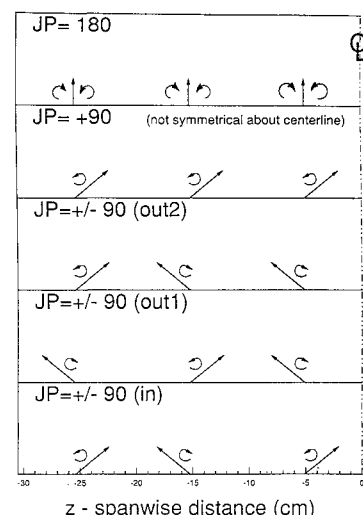


Fig. 3 Five configurations of VGJ jet directions as viewed downstream along the  $+x$  axis; curved arrows denote longitudinal vortex directions.

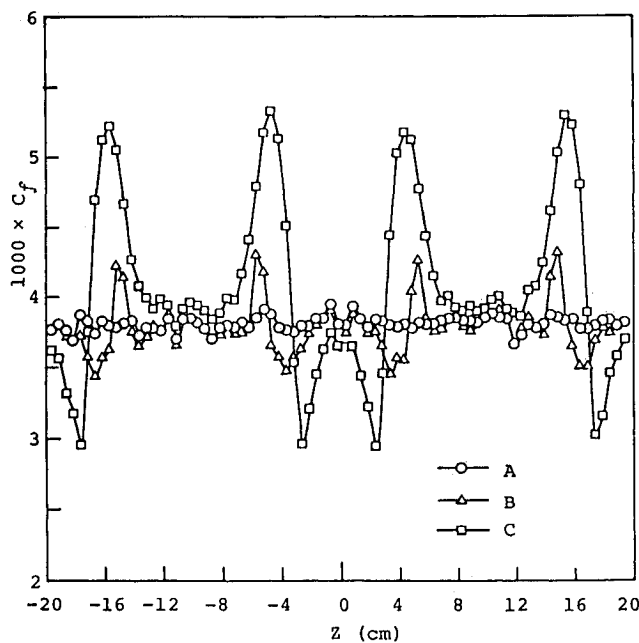


Fig. 4a Skin friction coefficient vs span [ $JP = \pm 90$  (in) configuration—at station L2]; curve A, no blowing (jetsoff); curve B,  $VR = 0.4$ , mild blowing; curve C,  $VR = 1$  strong blowing.

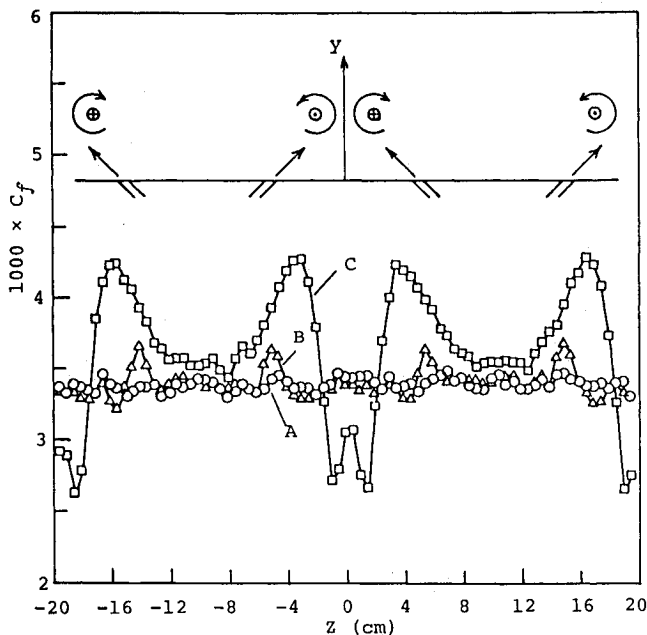


Fig. 4b Skin friction coefficient vs span [ $JP = \pm 90$  (in) at station L4]; curve A, no blowing (jetsoff); curve B,  $VR = 0.4$ ; curve C,  $VR = 1$ . Note: Sketch shows implied vortex centers and sense of rotation; wall jet locations at station L1; view is in  $+x$  direction looking downstream.

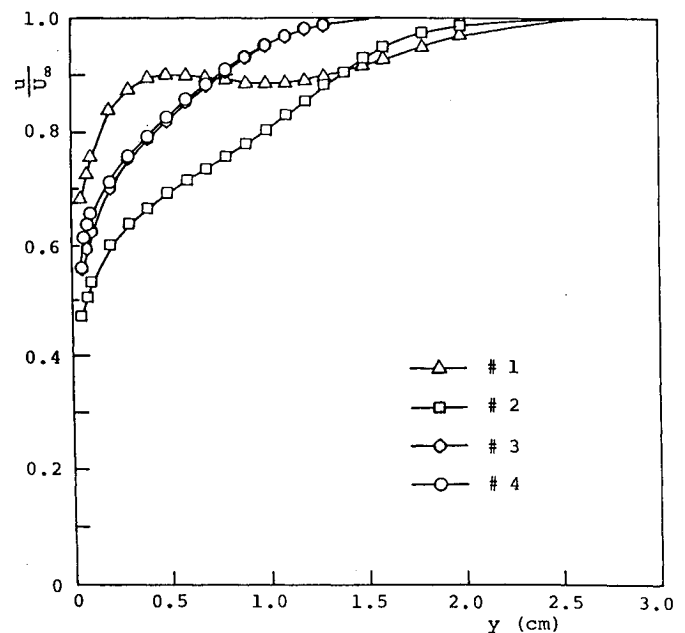


Fig. 5 Mean velocity profiles at station L2 for the  $JP = \pm 90$  (in) case with  $VR = 1$ ; curve 1 at maximum  $C_f$ ,  $z = -4.5$  cm; curve 2 at minimum  $C_f$ ,  $z = -2.5$  cm; curve 3,  $C_f$  at no blowing level,  $z = -10.5$  cm; no blowing, curve 7,  $z = 0$ .

It is also observed in these data that the  $C_f$  peaks located on opposite sides of the center plane move closer to each other from upstream at L2 to downstream at L4. This motion may result from two effects: 1) the spanwise convection of vortex cores resulting from residual spanwise momentum from the jets, and/or 2) core motion in response to mutual induction of the more closely spaced pairs, e.g., the central pair and their associated image vortices in the wall. The observed effect parallels results from a counter-rotating vortex array studied by Pauley and Eaton (see Fig. 10 in Ref. 7). They believe that mutual induction is the dominating effect. In any case, the observed spanwise migration in the  $C_f$  peaks in our data is consistent with the expected motions of a counter-rotating vortex pair near a wall.

To test the idea further that a VGJ actually creates a vortex, mean velocity profiles were taken at station L2 at selected  $z$  locations and the results compared to other results where vortices were definitely known to exist. The profiles for the  $VR = 1$  jet condition are shown in Fig. 5. Profile 1, the one with a velocity minimum near  $y = 1$  cm, is located at a point of maximum  $C_f$ , and 2, the slightly inflected profile, is at a point of minimum  $C_f$ . Profile 3 is located between the peaks, where  $C_f$  equals the  $C_f$  for the undisturbed layer. The shapes of these profiles correspond very closely with the shapes of similarly located profiles seen in solid vortex generator studies (e.g., Fig. 10 in Ref. 8). They can also be related to similar profiles in the early work of Wallis<sup>4</sup> where both VGJs and solid generators (pairs, closely spaced, and angled in the same direction) were compared, side by side, in a turbulent boundary layer. The velocity profiles reveal the reason for the peaks and valleys in skin friction. Fluid inflow on one side of a vortex imbedded in a boundary layer thins the inner region of the layer (below  $y = 1$  cm on curve 1, Fig. 5), which raises the local  $C_f$  with respect to its undisturbed value, and outflow on the other side of a vortex thickens the layer in this area and consequently lowers the local value of  $C_f$ .

The conclusion that longitudinal vortices are present seems unescapable at this point. For the case sketched in Fig. 6, with the jet pitched and skewed at angles  $\phi$  and  $\theta$ , our data suggests that the resulting longitudinal vortex will have its core vorti-

Figs. 8 and 9 in Ref. 8), a peak region of higher  $C_f$  was located under the vortex and to the side where the spanwise flow induced about the vortex center moved toward the wall, the region called the inflow zone. Conversely, a valley of low  $C_f$  was seen on the other side of a vortex under an outflow zone where flow is away from the wall. The sketch in the upper part of Fig. 4b, based on Pauley and Eaton's work, indicates the expected spanwise locations of the vortex cores at station L4 and indicates their rotations as one looks downstream. As in Fig. 3, short, straight arrows are drawn to indicate the upstream location and direction of the jets.

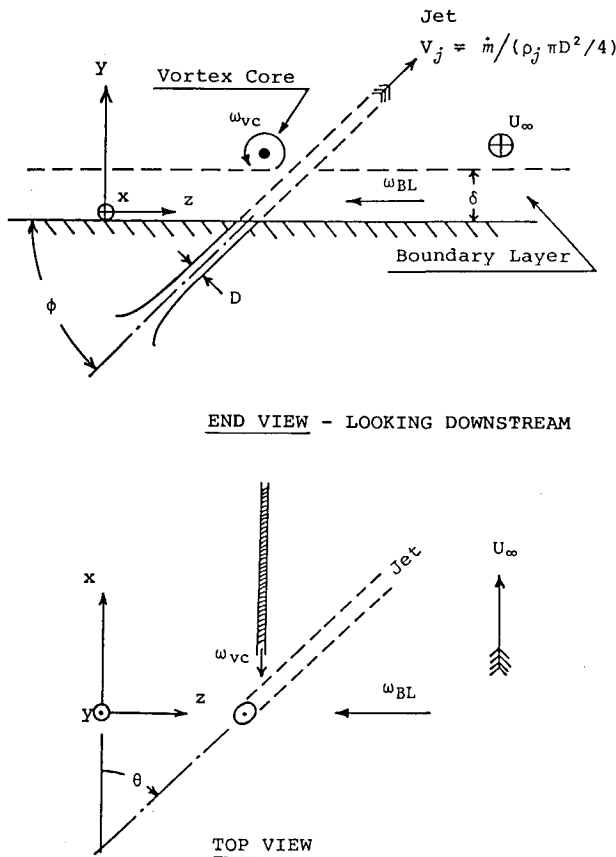


Fig. 6 General interpretation of a vortex generated by interaction of a pitched and skewed wall jet with a boundary layer.

city,  $\omega_{vc}$ , oriented as shown relative to the mean spanwise vorticity,  $\omega_{bl} = (U_\infty/\delta)$  in the approaching boundary layer. Since the vortices extend across the boundary layer and out into the freestream, see Fig. 5, they should be effective mixing agents for suppression of turbulent separation, and this proved to be the case in the proof-of-concept investigation, Set B described below.

The picture of a single vortex being produced by a skewed jet should be valid for a wide range of  $\theta$  angles. However, when  $\theta = 0$  or  $180$  deg, and possibly for a range of angles close to these values, two trailing longitudinal vortices of opposite sign should be produced by each jet as a result of the interaction of the jet with the boundary layer. Such vortex pairs are indicated in the sketch in Fig. 3 labeled  $JP = 180$ . Preliminary, detailed velocity field investigations downstream of a single VGJ shows that a vortex pair is produced for the  $180$  deg case, but measured secondary velocities (component in the  $y$ - $z$  plane) were much weaker than for a case where  $\theta = 90$  deg ( $VR = 1$  in both experiments). As shown in the Set B data below, the weaker vortex pairs generated by the  $JP = 180$  VGJ arrays were ineffective for separation control compared to the arrays that produce one strong vortex per jet. No experiments were conducted with jets pointed downstream,  $\theta = 0$  deg, because this configuration should produce even weaker vortices and poorer mixing than the  $180$ -deg case.

#### Set B

The results to show that the VGJ method can control separation and reduce stall rest on two types of experimental data. Figure 7 shows data on the percent of time the fluid layer at the wall (below  $y = 0.5$  mm and along the test section center-line) is in the forward or downstream direction. Figure 8 gives the corresponding streamwise distributions of the wall static pressure on the test surface. These results were obtained with the top wall deflected to create a diffuser-type flow with a strong adverse pressure gradient in the region of station L3 between  $x = 40$  and  $60$  cm. The dashed line in Fig. 1 shows the approximate top-wall setting for all cases.

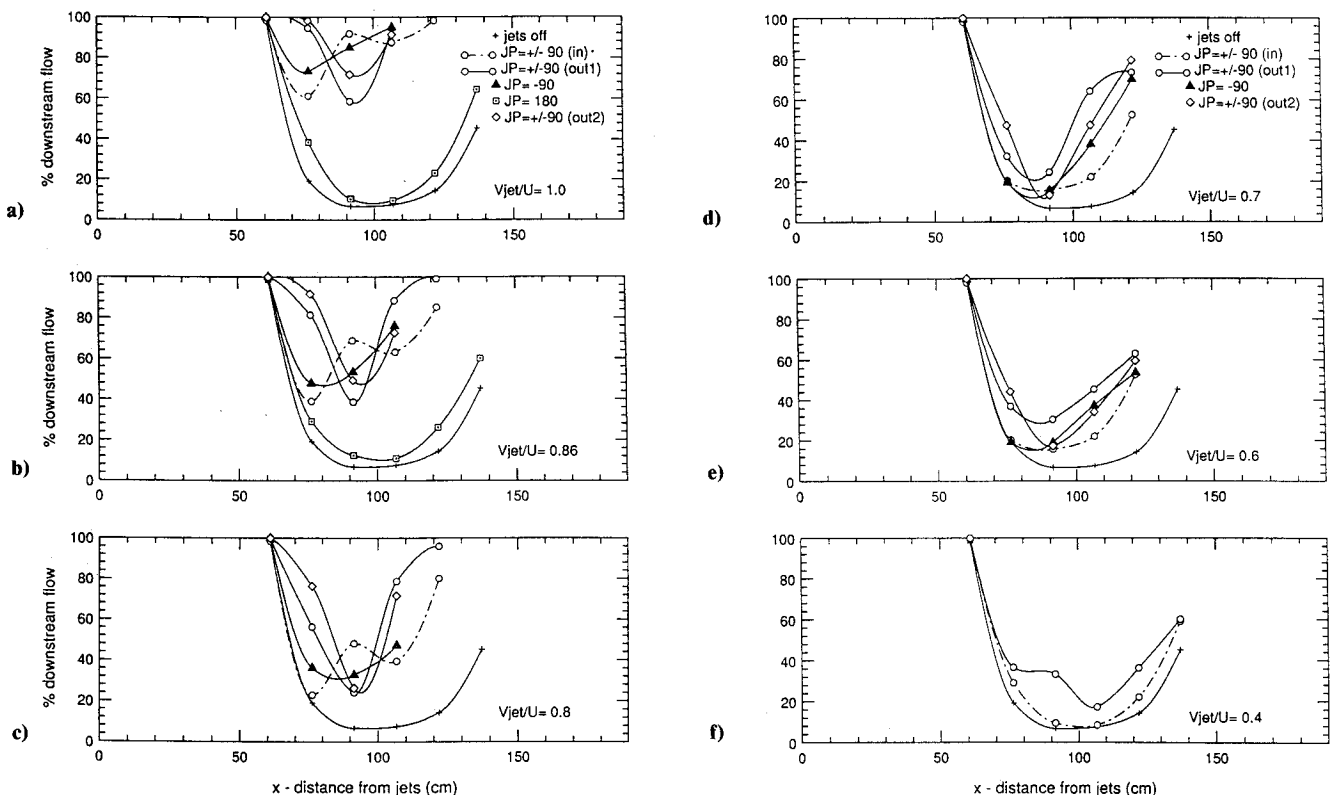


Fig. 7 Percent downstream flow at the wall (thermal tuft) vs distance downstream from the jets for six different velocity ratios,  $VR$ , compared to jets off case; see Fig. 3 for jet configurations.

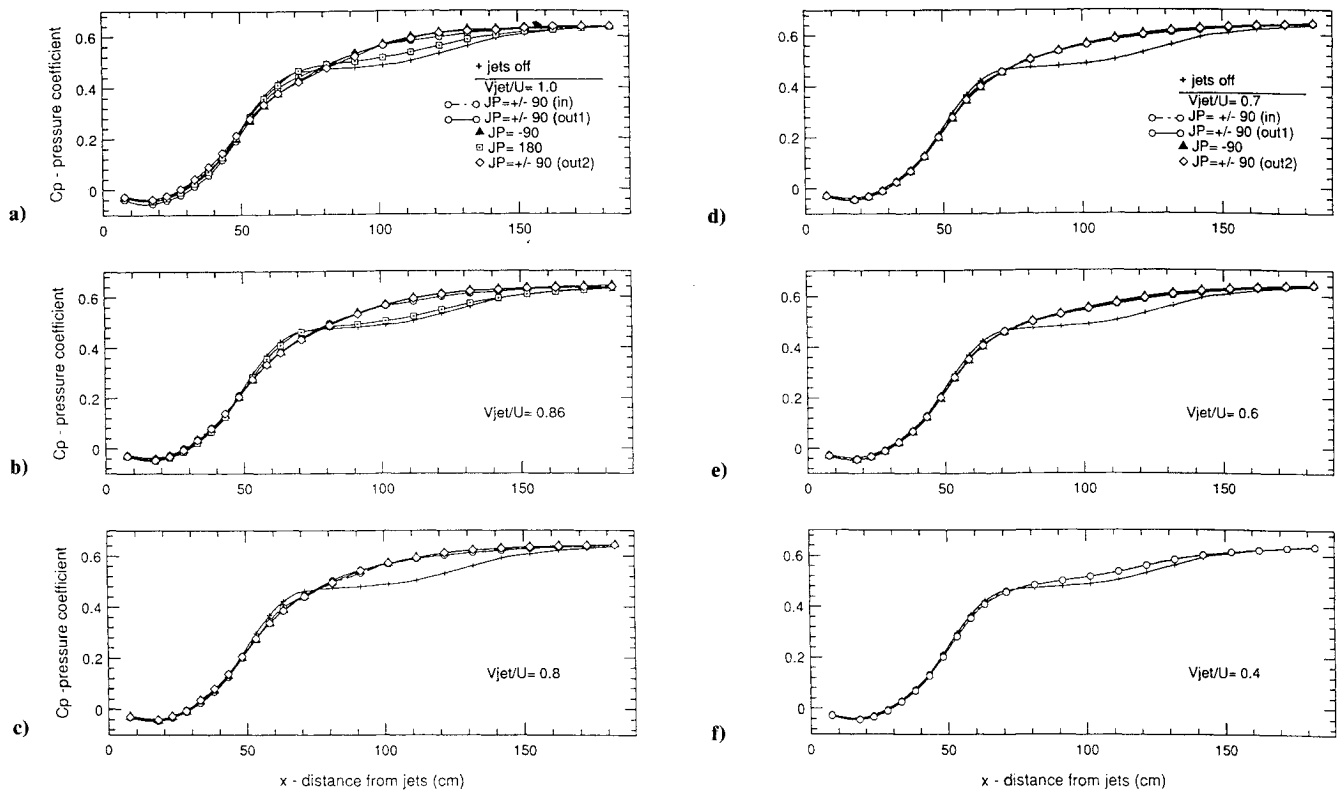


Fig. 8 Static pressure coefficient  $C_p = 2[p(x) - p_{ref}]/\rho U_{ref}^2$  vs distance downstream from the jets for six different velocity ratios  $VR$ ; ref evaluated at  $x = -3.8$  cm, slightly upstream of station L1.

Following the experiments whose results are described in Figs. 7 and 8, a second set of results on forward flow fraction and wall static pressure distribution were obtained with the region of strong adverse pressure gradient moved downstream to station L5. This was accomplished by deflecting the top wall upward with the same shape shown in Fig. 1 but translated downstream by two L stations, 61 cm. The results of these experiments were essentially identical to the original set B results. The conclusion that one can draw is that the cross-stream mixing effects are quite persistent because the vortices are persistent. This is supported in Figs. 4a and 4b by comparison of the peak amplitudes of  $C_f$  over an  $x$  distance of 61 cm. The  $C_f$  decays by 40%, but at the downstream station its peak is still significant for the case of  $VR = 1$ .

The results in Fig. 7 were obtained by application of an instrument referred to as the "thermal tuft," developed some years ago in our laboratory<sup>9</sup> by Eaton and co-workers. Its operation simulates a thread tuft, but it produces quantitative data. A fine wire, 6 mm long, is held across the axis of flow and 0.3 mm off the wall on short prongs. It is heated electrically; therefore its thermal wake moves upstream or down depending on the instantaneous wall-flow direction. The direction is detected on two fine platinum wires held parallel to the heater about 2.5 mm upstream and downstream, respectively. The detector wires, arranged in a bridge circuit, provide an instantaneous flow direction signal to a data acquisition computer. The wires are all part of a thermal tuft plug, which was flush mounted in ports at 15.2 cm intervals along the centerline of the test surface. Long time averages of the probe output gave the results shown in Fig. 7. No data were plotted at upstream ports where the flow is fully attached, 100% downstream flow.

A two-dimensional turbulent boundary layer is separated where percentage of time in downstream flow  $\gamma$  is 50% or less. A point of detachment (separation) is where  $\gamma = 50\%$  and  $\gamma$  is decreasing in the freestream direction. It has been shown in a number of experiments that mean wall skin friction is at or very close to zero where  $\gamma = 50\%$ . A point of reattachment exists where  $\gamma = 50\%$  and  $\gamma$  is increasing.

With the jets off (a line of reference in Figs. 7 and 8), one determines by these criteria that detachment starts at  $x = 68$  cm, and the flow reattaches at 138 cm, just downstream of the last data point of the jetsoff line in Fig. 7. The region of separation is 70 cm long, a substantial fraction of the test-section length. The static pressure distribution in Fig. 8 indicates that the stalled region must be quite thick because the curve of  $C_p(x)$  bends rapidly over at detachment ( $x = 68$  cm) and downstream of detachment  $C_p$  is nearly constant before it starts its slow increase ahead of reattachment at 138 cm. The boundary layers on the top wall and side walls of the duct forming the test section were probed with a small thread tuft and shown to be unseparated.

The  $JP = 180$  configuration is discussed separately below; for this unique case, the jets are not skewed. For the four cases with skewed jets, when the jets were operated at velocity ratios  $VR$  above 0.86, the test surface layer was unseparated, except for a small region where instantaneous backflows were seen a fraction of the time (see parts a and b of Fig. 7). The comparable  $C_p(x)$  profiles in parts a and b of Fig. 8 are quite different in shape from the jetsoff case. The shapes of the  $C_p$  curves in parts a and b are typical of unstalled or very mildly separated diffuser flows with thin separated regions. The degree of deviation of the  $C_p$  curves from the fully separated, jetsoff case is a qualitative measure of the size of the stalled region. Once  $VR$  drops below 0.8, the stalled region thickness and its length start to approach the jetsoff case. Figure 7 gives a good picture of the change in stalled region length and intensity as  $VR$  decreases. At  $VR = 0.4$ , the effects of the VGJs on stall size was negligible. The set A data in Fig. 4 also indicated weak vortex effects at  $VR = 0.4$ . For our test conditions, this appears to be the lower limit of utility, but a  $VR = 0.8$  need not be exceeded to reduce effectively the stalled region to a small size.

In the  $JP = 180$  configuration, all of the jets were pointing upstream,  $\theta = 180$  deg. Here we can see for the two cases of  $VR = 1$  and 0.86 that they were having almost no effect on the stalled region size or shape. As discussed already, this unique VGJ flow produced no substantial longitudinal vortices, at least none more effective than in the four skewed cases when

$VR=0.4$ . Skewed jets that produce single vortices appear to be the preferred geometries.

Finally, a comment or two concerning the results in Fig. 7 for the four skewed cases is needed. The (out 1) and (out 2) cases need not be considered separately. They are nearly identical and will be referred to simply as (out).

First, (out) should be contrasted to (in). Along the centerline, where the thermal tuft probe was used, these cases offer different flow situations. In the (out) cases, the vortices that span the center plane caused an inflow from freestream to the wall along the centerline. In the (in) case, the opposite was seen; wall fluid was convected away from the wall the centerline. Inflow should energize the layer and retard detachment and, outflow all along  $z=0$ , should have the opposite effect. This is indeed seen in Fig. 7; detachment was moved downstream for the (out) cases. For the (in) case, which produces outflow along the centerline, detachment location is hardly affected for any velocity ratio. As a result of these observations, one may picture the spanwise average detachment line moved downstream, but across the span there is a periodic upstream and downstream waviness to lines of constant percentage downstream flow. Interestingly, the case where all vortices corotate,  $JP=90$ , lay between (in) and (out) and also show some downstream movement of detachment for  $VR>0.8$ .

The (out)-(in) trends seen near detachment reverse completely in the center of the stalled region. The reason for this is yet to be explained, but it may be associated with the merging or interaction of counter-rotating vortex pairs. Nevertheless, it is thought that the case of  $JP=90$  represents the spanwise mean effect for either (in) or (out). Thus, considering spanwise mean effects only, it appears that the length of the stalled region is more strongly affected by bringing the reattachment point forward than by pushing detachment downstream. This may be a consequence of our particular flow configuration and should not be generalized.

### Conclusions

Vortex generator jets are shown to produce longitudinal streamwise vortices in the downstream direction in a turbulent boundary layer, and these vortices are sufficiently strong, under the proper circumstances, to substantially reduce and nearly eliminate a large stalled region of turbulent separated flow.

More specifically, within the confines of our apparatus and flow conditions, it was shown that 1) for skewed jets, substan-

tial stalled region size reduction occurs for jet velocity ratios  $VR$  above 0.8, 2) skewed jets are effective, but jets that point directly upstream are ineffective, 3) jet arrays that give counter rotating vortex pairs can cause significant spanwise variations, and 4) spanwise average reattachment location seems more strongly affected than detachment location, at least for our conditions.

### Acknowledgments

We thank the Air Force Office of Scientific Research for the "Flow Control" University Research Initiative (URI) grant and the Industrial Affiliates of the Thermosciences Division for support of the program. A grant from the government of Japan supported M. Nishi during his visit. Dan Coffey assisted ably in the Set B experiments.

### References

- <sup>1</sup>Pearcey, H. H., "Shock Induced Separation and its Prevention," *Boundary Layer & Flow Control*, Vol. 2, edited by G. V. Lachmann, Pergamon, New York, 1961, pp. 1170-1344.
- <sup>2</sup>Wallis, R. A., "The Use of Air Jets for Boundary Layer Control," Aerodynamics Research Laboratories, Australia, Aero Note 110, (N-34736), 1952.
- <sup>3</sup>Wallis, R. A., and Stuart, C. M., "On the Control of Shock-Induced Boundary-Layer Separation with Discrete Jets," Aeronautical Research Council, Australia, Current Paper No. 595, (N63-10138), 1958.
- <sup>4</sup>Wallis, R. A., "A Preliminary Note on a Modified Type of Air Jet for Boundary Layer Control," Aeronautical Research Council, Australia, Current Paper No. 513, 1960.
- <sup>5</sup>Ball, W. H., "Tests of Wall Blowing Concepts for Diffuser Boundary Layer Control," AIAA Paper 84-1276, June 1984.
- <sup>6</sup>Patel, V. C., "Calibration of the Preston Tube and Limitations on its use in Pressure Gradients," *Journal of Fluid Mechanics*, Vol. 23, Sept. 1965, pp. 185-208.
- <sup>7</sup>Pauley, W. R., and Eaton, J. K., "Experiments on the Development of Longitudinal Vortex Pairs Embedded in a Turbulent Boundary Layer," *AIAA Journal*, Vol. 26, No. 7, July 1988, pp. 816-823.
- <sup>8</sup>Pauley, W. R., and Eaton, J. K., "The Effects of Embedded Longitudinal Vortex Pairs on Turbulent Boundary Layer Heat Transfer," *Transport Phenomena in Turbulent Flows*, edited by M. Hirata and N. Kasagi, Hemisphere, New York, 1988, pp. 487-500.
- <sup>9</sup>Eaton, J. K., Johnston, J. P., Jeans, A. H., and Ashjaee, J., "A Wall-Flow-Direction Probe for Use in Separating and Reattaching Flows," *Transactions of the ASME, Journal of Fluids Engineering*, Vol. 101, No. 3, Sept. 1979, pp. 364-308.